THE JOURNAL OF BIOLOGICAL CHEMISTRY
Vol. 272, No. 46, Issue of November 14, pp. 29158–29166, 1997

Printed in U.S.A.

Mouse Mast Cell Protease 9, a Novel Member of the Chromosome 14 Family of Serine Proteases that is Selectively Expressed in Uterine Mast Cells*

(Received for publication, April 15, 1997, and in revised form, June 10, 1997)

John E. Hunt‡§, Daniel S. Friend¶, Michael F. Gurish‡, Eric Feyfant‖, Andrej Šali‖, Chifu Huang‡, Namit Ghildyal‡, Stephen Stechschulte‡, K. Frank Austen‡, and Richard L. Stevens‡§§**

From the Departments of ‡Medicine and ¶Pathology, Harvard Medical School, Boston, Massachusetts 02115, the ¶Department of Pathology and the ‡Division of Rheumatology, Immunology, and Allergy, Brigham and Women's Hospital, Boston, Massachusetts 02115; and ‖the Rockefeller University, New York, New York 10021

Mouse mast cell protease (mMCP) 1, mMCP-2, mMCP-4, and mMCP-5 are members of a family of related serine proteases whose genes reside within an ~850 kilobase (kb) complex on chromosome 14 that does not readily undergo crossover events. While mapping the mMCP-1 gene, we isolated a novel gene that encodes a homologous serine protease designated mMCP-9. The mMCP-9 and mMCP-1 genes are only ~7 kb apart on the chromosome and are oriented back to back. The proximity of the mMCP-1 and mMCP-9 genes now suggests that the low recombination frequency of the complex is due to the closeness of some of its genes. The mMCP-9 transcript and protein were observed in the jejunal submucosa of *Trichinella spiralis*-infected BALB/c mice. However, in normal BALB/c mice, mMCP-9 transcript and protein were found only in those mast cells that reside in the uterus. Thus, the expression of mMCP-9 differs from that of all other chymases. The observation that BALB/c mouse bone marrow-derived mast cells developed with interleukin (IL) 10 and c-*kit* ligand contain mMCP-9 transcript, whereas those developed with IL-3 do not, indicates that the expression of this particular chymase is regulated by the cytokine microenvironment. Comparative protein structure modeling revealed that mMCP-9 is the only known granule protease with three positively charged regions on its surface. This property may allow mMCP-9 to form multimeric complexes with serglycin proteoglycans and other negatively charged proteins inside the granule. Although mMCP-9 exhibits a >50% overall amino acid sequence identity with its homologous chymases, it has a unique substrate-binding cleft. This finding suggests that each member of the chromosome 14 family of serine proteases evolved to degrade a distinct group of proteins.

A closely linked complex of genes that encode mouse mast cell protease (mMCP)[1] 1, mMCP-2, mMCP-4, mMCP-5, cathepsin G, and granzymes B to G exists on chromosome 14 (1–5). Relative to pancreatic chymotrypsin, these serine proteases have a conserved set of insertions and deletions in their amino acid sequences. The three-dimensional structure of rat mast cell protease II (rMCP-II), which was determined by x-ray crystallography (6), shows that the changes result in subtle but important differences relative to the chymotrypsin structure. The deletion of a Cys residue, and therefore a disulfide bond, in the C-terminal portion of these proteases represents one of the amino acid sequence changes that causes a prominent loop to extend part way into the substrate-binding cleft (6, 7). It is believed that this structural feature causes the chromosome 14 family of serine proteases to have substrate specificities that are more restricted than that of chymotrypsin, whose homologous gene resides on chromosome 8.

Each of these serine proteases appears to have a unique set of amino acids in its substrate-binding cleft. It is conceivable that the mMCP genes evolved on chromosome 14 because of the need for multiple proteases with restricted but different substrate specificities. For example, granzyme B is so similar to pancreatic chymotrypsin in its overall amino acid sequence that it was originally predicted to be a chymase. However, granzyme B actually prefers an Asp residue at the P1 position of its substrates because the S1 site of this protease includes the Arg^{207} residue (8). Thus, it appears that the consequence of restricted substrate specificity led to evolutionary pressure for a larger number of related genes in the mouse.

mMCP-1, mMCP-2, mMCP-4, and mMCP-5 all have a conserved face on their surfaces away from the substrate-binding cleft that is positively charged (7) at the granule pH of 5.5 (9). It is believed that this positively charged region enables these chromosome 14 chymases to interact electrostatically with negatively charged serglycin proteoglycans in the Golgi region, ensuring the targeting of only properly folded proteases to the secretory granule and the accurate proteolytic conversion of the zymogens after sequestration in the intracellular storage com-

* This work was supported by National Institutes of Health Grants AI-07306, AI-22531, AI-23483, AI-31599, AR-07530, AR-36308, GM-54762, HL-48598, and HL-36110 and by a Sinsheimer Scholar Award (to A. S.). The costs of publication of this article were defrayed in part by the payment of page charges. This article must therefore be hereby marked "*advertisement*" in accordance with 18 U.S.C. Section 1734 solely to indicate this fact.

The nucleotide sequence(s) reported in this paper has been submitted to the GenBank™/EBI Data Bank with accession number(s) AF007119 and AF007120.

§ Recipient of a C. J. Martin Fellowship from the National Health and Medical Research Council of Australia.

** Recipient of a fellowship from Association pour le Development de l'Enseignement et des Recherches pour la Region Provence-Alpes-Cote D'Azur.

§§ To whom correspondence should be addressed: Brigham and Women's Hospital, Smith Building, Rm. 616B, 75 Francis St., Boston, MA 02115. Tel.: 617-525-1231; Fax: 617-525-1310; E-mail: rstevens@rics.bwh.harvard.edu.

[1] The abbreviations used are: mMCP, mouse mast cell protease; bp, base pair(s); Ig, immunoglobulin; IL, interleukin; kb, kilobase; KL, c-*kit* ligand; mBMMC, mouse bone marrow-derived mast cells; mMC-CPA, mouse mast cell carboxypeptidase A; PBS, phosphate-buffered saline; PCR, polymerase chain reaction; rMCP, rat mast cell protease; RT, reverse transcriptase.

partment. The tryptase mMCP-7 (10, 11), whose gene resides on chromosome 17 rather than chromosome 14, also possesses the conserved face, but its proteoglycan-binding domain includes several His residues in addition to the Lys and Arg residues (12). The tryptase mMCP-6 (13), whose gene also resides on chromosome 17, is an exception in that its putative proteoglycan-binding domain resides on a different part of the molecular surface (14). The electrostatic characteristics of these proteoglycan-binding domains are important for functional diversity among the mMCPs because they determine both the equilibrium concentration and the rate at which the various chymases and tryptases dissociate from the exocytosed granule core (14).

The mMCP-1, mMCP-2, mMCP-4, and mMCP-5 genes are each ~3 kilobases (kb) in size and contain 5 exons (3, 15–17). Pulse-field gel electrophoresis revealed that they are located on an ~850-kb fragment of chromosome 14, but mapping studies failed to reveal a crossover point in the complex even when the linkage analysis was extended to the chromosome 14 family of granzyme genes (2, 3). Thus, either many of the protease genes are quite close in the complex or some structural constraint in this region of chromosome 14 hinders recombination events.

Because knowledge concerning the order and orientation of the members of the chromosome 14 family of serine protease genes and the relative distances between them is needed for an understanding of their transcriptional regulation, we and others have begun to map the genomic complex in the mouse. We now describe a novel gene, mMCP-9, that resides only ~7 kb away from the mMCP-1 gene on chromosome 14. The proximity of the two chymase genes offers an explanation for the low recombination frequency of the chromosome 14 complex of serine protease genes. We also show that the mMCP-9 gene, its transcript, and its translated product have several interesting features that account for the selective expression of this gene in specific populations of mast cells.

EXPERIMENTAL PROCEDURES

Cloning and Nucleotide Sequencing of the mMCP-9 Gene—A λ bacteriophage clone (JH-1) (see Fig. 1A) was isolated by screening a BALB/c mouse genomic library under conditions of high stringency with a radiolabeled probe specific for the mMCP-1 gene (15). Mapping analysis with varied restriction enzymes revealed that clone JH-1 contained two homologous but distinct genes. Thus, with standard methodologies, the three *Eco*RI-derived fragments liberated from the insert were subcloned into Bluescript, and their nucleotide sequences were determined with dideoxy/cycle sequencing methodologies (18). One sequence corresponded to the mMCP-1 gene. Because the other was novel, it was designated the mMCP-9 gene.[2] A polymerase chain reaction (PCR) approach confirmed that the *Eco*RI fragments were contiguous in the phage clone. For example, mMCP-9-specific sense (5′-GTACATCTTGCCTCCAAATTAC-3′) and antisense (5′-CAACACATCGCCCAGGCTT-3′) primers were used to amplify a 300-base pair (bp) fragment from the clone that spanned the *Eco*RI site between fragments JH-1B and JH-1C. Each of the 30 cycles of the PCR consisted of a 30-s denaturing step at 94 °C, a 45-s annealing step at 60 °C, and a 60-s extension step at 72 °C. Generally, each PCR contained 50 ng of phage DNA and 300 ng of primer in a total reaction volume of 100 μl. The amplified products were subjected to electrophoresis in a 0.8% low melting point agarose gel, and the appropriate DNA fragments were excised, purified with Geneclean™ (BIO 101 Inc., Vista, CA), and sequenced.

The orientation and spacing of the mMCP-1 and mMCP-9 genes in chromosomal DNA were confirmed with a long range PCR approach.

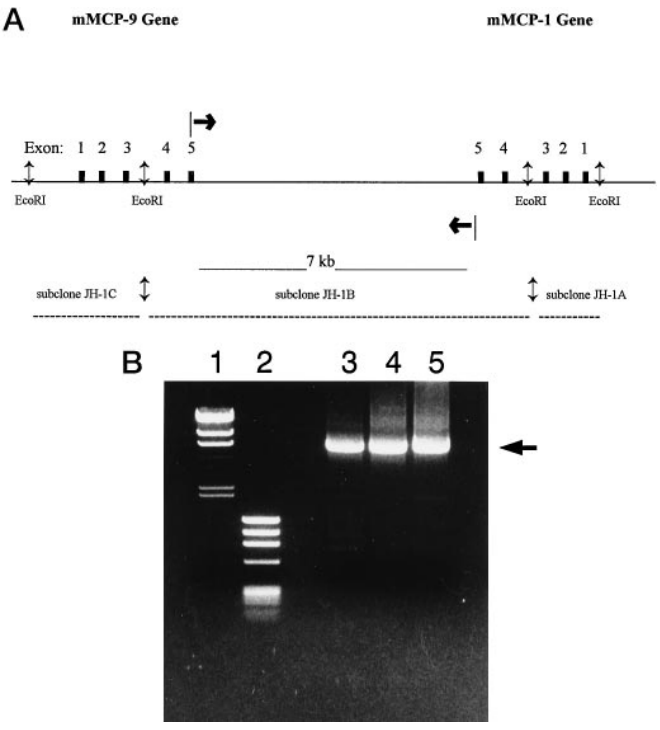

FIG. 1. **Organization of the mMCP-1 and mMCP-9 genes on chromosome 14.** Although not drawn to scale, the map of the λ phage clone JH-1 is depicted in *panel A*. The five exons of each gene in the insert are *boxed* and *numbered*. The *vertical double arrows* (↕) indicate the *Eco*RI-susceptible sites in the insert. The *horizontal bold arrows* (→) in panel *A* indicate the location of the primers used in the long range PCR of chromosomal DNA depicted in *panel B*. In *panel B*, template DNA was derived from BALB/c chromosomal DNA (*lane 3*), the entire JH-1 phage clone (*lane 4*), or its subcloned fragment JH-1B (*lane 5*). *Lanes 1* and *2* contain fragments obtained from a *Hin*dIII digest of λ DNA and a *Hae*III digest of φX174 DNA, respectively. The *arrow* on the *right* refers to the PCR-generated fragment.

Each 100-μl sample contained 200 ng of BALB/c mouse chromosomal DNA (CLONTECH), 300 ng of an oligonucleotide primer (5′-TTCACCCCAATCTCCCCAC-3′) that corresponded to a region in exon 5 of the mMCP-9 gene, and 300 ng of an oligonucleotide primer (5′-CCTGTCCCTTTGAGGATCTCA-3′) that corresponded to a region in exon 5 of the mMCP-1 gene. A long range PCR kit was used according to the recommendations of the manufacturer. Each of the 30 cycles of the PCR consisted of a 1-min denaturing step at 94 °C, a 10-min annealing step at 60 °C, and a 10-min extension step at 72 °C.

Isolation and Characterization of the mMCP-9 Transcript in Different Tissues—The mMCP-9 transcript was sought in various tissues of normal BALB/c mice (The Jackson Lab., Bar Harbor, ME), BALB/c mice that had been infected with *Trichinella spiralis* (20, 21), BALB/c mice that had a systemic mastocytosis following the adoptive transfer of the V3 mast cell line (22), and in *in vitro* derived BALB/c mast cells (23, 24). RNA was isolated according to the method of Chomczynski and Sacchi (25) from liver, spleen, ear, intestine, and uterus of normal BALB/c mice and from liver and spleen of V3 mastocytosis mice. V3 mastocytosis mice were used 2–4 weeks after the adoptive transfer of ~10^6 v-*abl*-immortalized V3 mast cells into the tail vein of each 6-week-old BALB/c mouse (22). RNA also was isolated from mouse bone marrow-derived mast cells (mBMMC) that were developed for 3 weeks with recombinant mouse interleukin-3 (IL) (100 units/ml) alone (23) or 5 weeks with both recombinant mouse c-*kit* ligand (KL) (100 ng/ml) and IL-10 (100 units/ml) (24). Lastly, BALB/c mice were infected with ~500 *T. spiralis* larvae (20, 21), and then total RNA was isolated from the intestine on day 10 after infection.

Based on the nucleotide sequence of the mMCP-9 gene, including its exon/intron organization, primers were designed for reverse transcriptase (RT) PCR that would enable the amplification and cloning of an ~650-bp cDNA that encodes from residues 17 to 226 of mature mMCP-9. Reverse transcription was performed on 5 μg of total RNA with avian myeloblastoma virus RT (Invitrogen, San Diego, CA). The reaction was oligo(dT)-primed, and two cycles were performed at 42 °C, each for 1 h. PCR was then performed with sense (5′-TGGCCTATGT-

[2] The novel gene was designated as the mMCP-9 gene because it is the ninth granule serine protease expressed by mouse mast cells. Although the N-terminal amino acid sequence of mMCP-3 has been determined (19), the nucleotide sequence of its transcript and that of its gene have not. The nucleotide and deduced amino acid sequences of the mMCP-8 transcript have been reported by Huang and co-workers in GenBank™ Data Bank (accession number X78545). The GenBank accession numbers for the mMCP-9 gene and cDNA are AF007119 and AF007120, respectively.

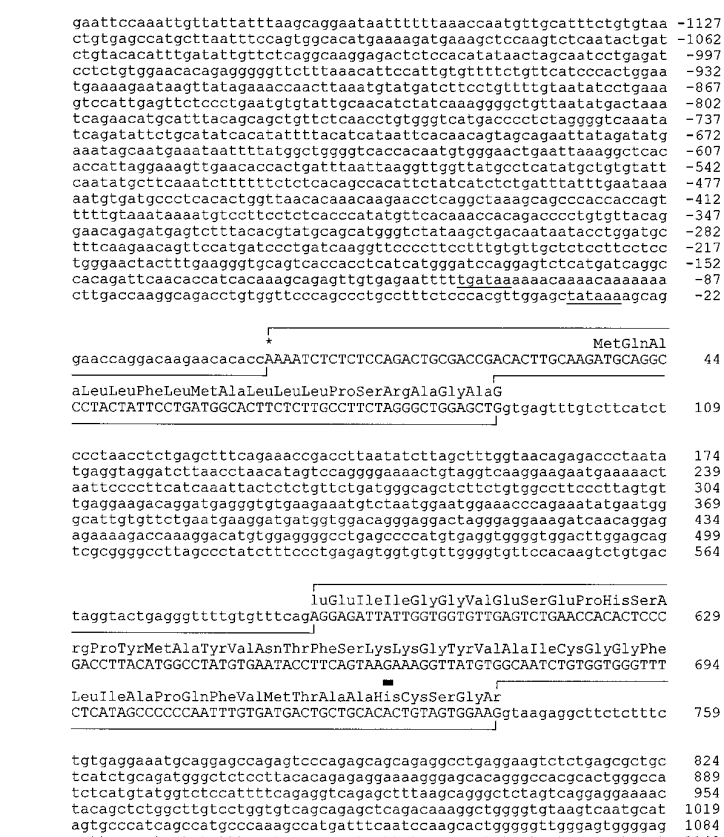

FIG. 2. **Structure of the mMCP-9 gene.** Nucleotides comprising introns are in *lowercase letters*, and those comprising exons in *uppercase letters*. The exons are *boxed*. The TATA box and GATA-binding motif 5′ of the putative transcription initiation site are *underlined*. The polyadenylation regulatory signal is *double underlined*. The components of the catalytic triad (■) are indicated. Numbering begins at the putative transcription-initiation site (*).

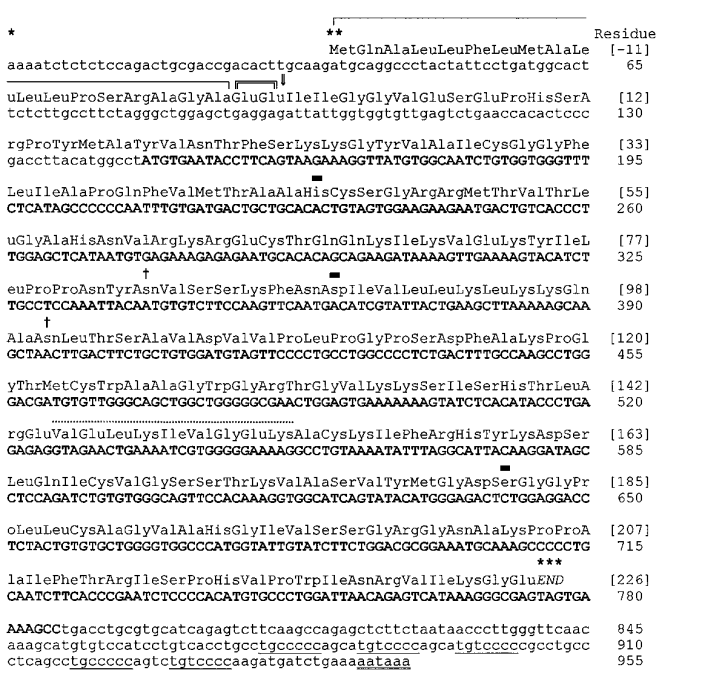

FIG. 3. **Nucleotide sequence of a mMCP-9 cDNA and its predicted amino acid sequence.** An RT-PCR approach was used to obtain a near full-length (*bold uppercase letters*) mMCP-9 cDNA from the intestines of *T. spiralis*-infected BALB/c mice. The remainder of the mMCP-9 transcript (*lowercase letters*) was deduced by comparing the portions of its genomic sequence with homologous mMCP-1 (20), mMCP-2 (36), mMCP-4 (16), and mMCP-5 (17) transcripts. The two potential *N*-linked glycosylation sites (†), components of the catalytic triad (■), putative transcription-initiation site (*), translation-initiation site (**), translation-termination signal (***), 18-mer signal peptide (*single overhead bracket*), Glu-Glu activation peptide (*double overhead bracket*), 9-mer peptide used to obtain the mMCP-9-specific antibody (. . . . .), *UGXCCCC* motifs in the 3′-UTR (*underlined*), and polyadenylation regulatory sequence (*double underlined*) are indicated. Nucleotide numbering begins at the putative transcription-initiation site. Amino acid numbering (*within brackets* at *right*) begins with residue 1 of the mature protein. The *arrow* (⇓) indicates the predicted cleavage site of the signal peptide.

GAATACCTTCAGTAA-3′) and antisense (5′-GGCTTTTCACTACTC-GCCCTT-3′) primers specific for mMCP-9 or sense (5′-GTGGGC-CGCTCTAGGCACCAA-3′) and antisense (5′-CTCTTTGATGTCACG-CACGATTTC-3′) primers (CLONTECH) specific for mouse cytoplasmic β-actin (26). Each of the 30 cycles of the PCR consisted of a 1-min denaturing step at 94 °C, a 2-min annealing step at 60 °C, and a 3-min extension step at 72 °C. Vent polymerase was used to reduce the number of PCR-induced point mutations in the nucleotide sequences of the generated DNA. The RT-PCR products were electrophoresed on a 1% agarose gel containing ethidium bromide, and their sizes were determined by comparison with fragments obtained from a *Hin*dIII digest of λ DNA, a *Hae*III digest of *ϕ*X174 DNA, or a synthetic DNA ladder consisting of 15 blunt-ended fragments that increase in multiples of 100 bp from 100 to 1500 bp (Life Technologies, Inc., Gaithersburg, MD). In one instance, the RT-PCR product obtained from the intestine of *T. spiralis*-infected mice was purified, inserted into a PCR cloning vector with a commercially available kit (5 Prime → 3 Prime, Inc., Boulder, CO), and sequenced. In another instance, the RT-PCR product from uterus was purified by gel electrophoresis and directly sequenced.

Generation and Use of an Anti-peptide Antibody That Selectively Recognizes mMCP-9—An immunohistochemical approach (27) was used to evaluate the presence of mMCP-9 protein in different populations of *in vivo* differentiated mast cells. The peptide Val-Glu-Leu-Lys-Ile-Val-Gly-Glu-Lys, which corresponds to residues 144 to 152 of mature mMCP-9, is not present in homologous mMCP-1, mMCP-2, mMCP-4, or mMCP-5. A model of the three-dimensional structure of

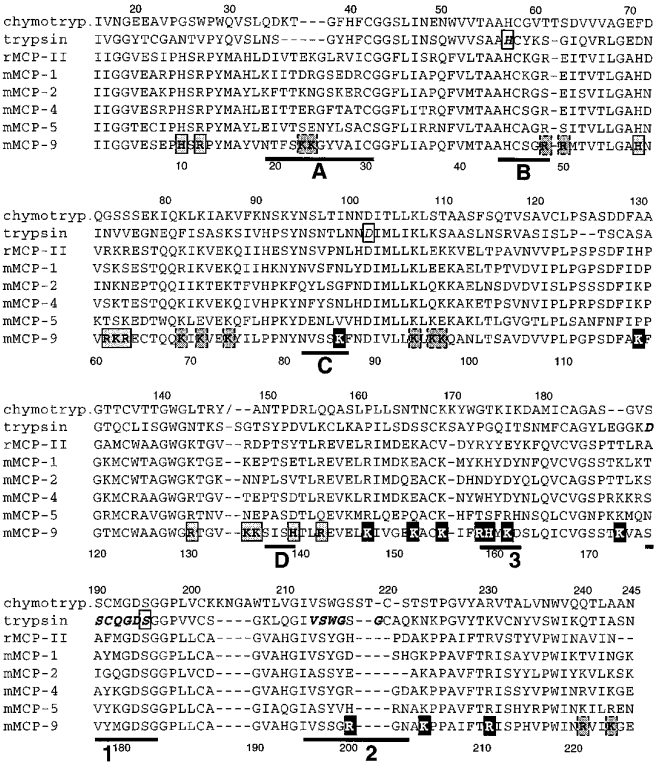

FIG. 4. **Comparison of the deduced amino acid sequence of mature mMCP-9 with related serine proteases.** The alignments of mMCP-9 with mMCP-1 (37), mMCP-2 (36), mMCP-4 (16), mMCP-5 (17), rMCP-II (38), bovine pancreatic trypsin (39), and bovine pancreatic chymotrypsin A (40) were calculated by MODELLER (31) and edited by hand to shift several gaps into a more appropriate structural context. The seven major loops defining the substrate-binding cleft in trypsin-like serine proteases (41) are underlined (*A, B, C, D, 3, 1,* and *2)*. Each substrate-binding subsite within the cleft is formed by one or more of these loops. The three positively charged regions are indicated (region 1, *white letters in black boxes*; region 2, *dashed lines around shaded boxes*; region 3, *continuous lines around shaded boxes*). The 14 residues in the S1 site of trypsin that have at least one atom within 4.5 Å of any atom of the P1 Lys residue in bovine pancreatic trypsin inhibitor (Brookhaven National Laboratory Protein Data Bank code 2PTC) are shown in *bold italic* style. The three active site residues in trypsin, His^{57}, Asp^{102}, and Ser^{195}, are indicated. The *numbers* in the *top* and *bottom lines* refer to the residues in chymotrypsin and mMCP-9, respectively.

homologous chymase mMCPs (7) predicted that this peptide would protrude from the surface of the folded enzyme. Thus, antibodies were raised in rabbits against the synthetic peptide by Quality Controlled Biochemicals (Hopkinton, MA). An enzyme-linked immunosorbent assay (ELISA) with peptide coupled to bovine serum albumin detected reactivity at an ~30,000-fold dilution. When SDS-PAGE/immunoblot analysis was used to test its specificity, the affinity-purified antibody at a 1000-fold dilution did not recognize insect cell-derived recombinant mMCP-1, mMCP-2, mMCP-4, or mMCP-5 (data not shown).

Immunohistochemistry was carried out as described for anti-peptide antibodies to mMCP-1 (21), mMCP-2 (28), mMCP-4,[3] and mMCP-5 (29). Sections of tissue were fixed in 4% paraformaldehyde in phosphate-buffered saline (PBS) for 4 h at room temperature, dehydrated, embedded in JB4 glycolmethacrylate (Polysciences Inc., Warrington, PA), sectioned at 2 μm thickness, and picked up on glass slides. In each analysis, the chloroacetate esterase enzyme cytochemistry reaction (21, 30) was performed on the first serial section to identify all chymase-positive mast cells. The rest of the slides were routinely incubated sequentially in 2 mM $CaCl_2$ containing 0.125% trypsin, PBS containing 0.05% Tween-20 and 0.1% bovine serum albumin, PBS containing 0.05% Tween-20 and 4% normal goat serum, and 4% normal goat serum containing the appropriate affinity purified rabbit immunoglobulin (Ig). The samples were washed, incubated in buffer containing biotin-labeled goat anti-rabbit IgG, washed twice in 0.1% bovine serum albumin and

[3] N. Ghildyal and R. L. Stevens, unpublished data.

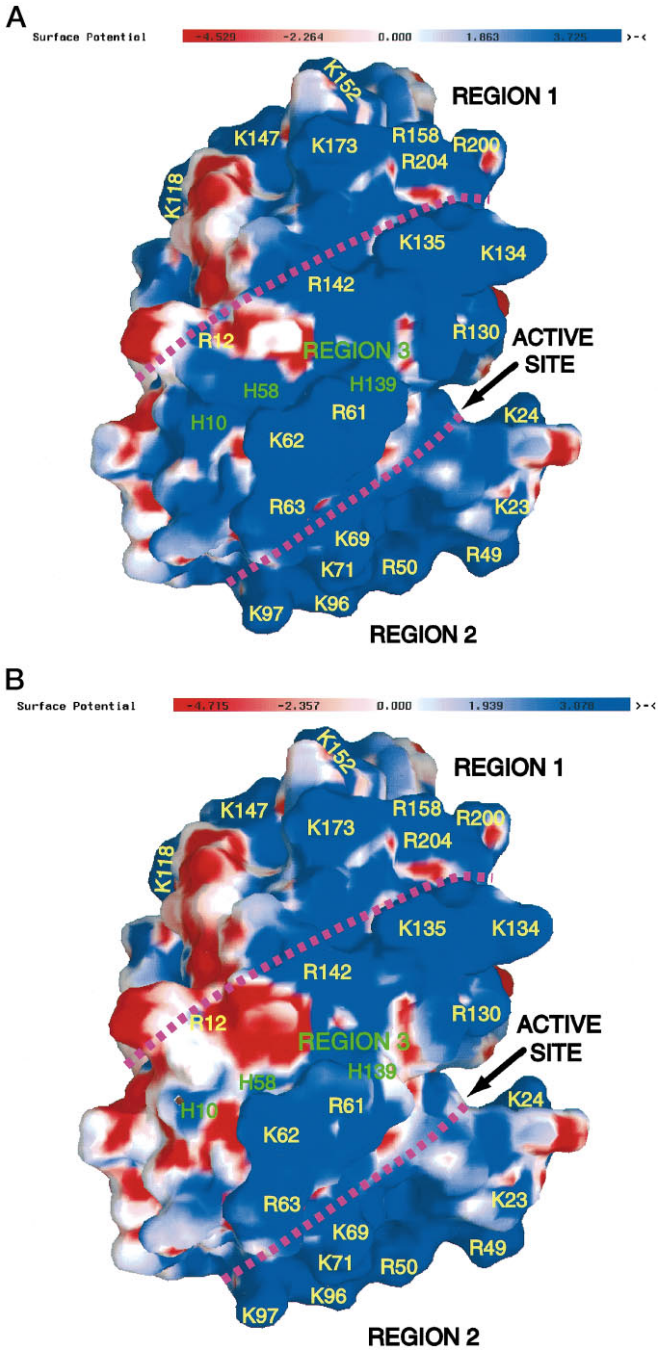

FIG. 5. **Electrostatic potential for the three-dimensional model of mMCP-9 below (*A*) and above (*B*) pH 6.5.** The electrostatic potential on the molecular surface of mMCP-9 was calculated and displayed with program GRASP (34), with use of the ionic strength of 150 mM and the relative dielectric constants of 2 and 78 for protein and solvent, respectively. The electrostatic potential is colored according to the depicted *color bar* at the *top* of each *panel* (in units of kT; 1 kT unit = 0.58 kcal/electron mole). The *blue* and *red* colored *patches* on the surface of the molecule correspond to the regions with a net concentration of positive and negative charges, respectively. Each His residue has a single positive charge in *panel A* and no charge in *panel B*. His residues are labeled in *green*, Arg and Lys residues in *yellow*. In the depicted orientation of mMCP-9 with its substrate-binding cleft located on the *far right*, positively charged regions 1, 2, and 3 are located on the *top*, *bottom*, and *middle*, respectively. Positively charged residues Lys^{86}, Lys^{155}, His^{159}, Lys^{161}, and Arg^{211} in region 1 and Lys^{74}, Lys^{94}, Arg^{221}, and Lys^{224} in region 2 are not visible in this orientation. The boundaries between the regions are indicated by two *pink dashed lines*. The depicted orientation is similar to that used previously for mMCP-4 (7), mMCP-6 (14), and mMCP-7 (12).

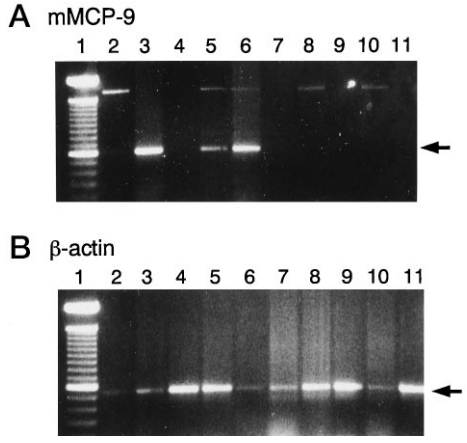

FIG. 6. **Expression of the mMCP-9 transcript in tissues and cultured mast cells.** An RT-PCR approach was used to monitor the presence of the mMCP-9 transcript in normal and diseased tissues and cultured mast cells (*A*). The presence of mMCP-9 transcript was evaluated in the intestine (*lane 2*), uterus (*lane 6*), ear (*lane 7*), liver (*lane 8*), and spleen (*lane 9*) of normal BALB/c mice; the intestine of *T. spiralis*-infected BALB/c mice (*lane 3*); BALB/c mBMMC developed *in vitro* with IL-3 (*lane 4*); BALB/c mBMMC developed *in vitro* with of IL-10 and KL (*lane 5*); and liver (*lane 10*) and spleen (*lane 11*) of the V3 mastocytosis mouse. Depicted in *lane 1* is a synthetic DNA ladder, consisting of 15 blunt-ended fragments that increase in multiples of 100 bp from 100 to 1500 bp. For positive controls, RT-PCRs were performed with β-actin-specific primers (*B*). The *arrows* indicate mMCP-9 and β-actin RT-PCR products. Nucleotide sequence analysis confirmed that the RT-PCR product generated from uterus mRNA encodes mMCP-9. Because the primers used in the RT-PCR assay correspond to nucleotide sequences that reside in exons 2 and 5 of the mMCP-9 gene, the larger sized fragments depicted in *lanes 2*, *5*, *6*, *8*, and *10* of *panel A* are the intron-containing products derived from residual genomic DNA.

0.05% Tween-20 in PBS, incubated in Vectastain ABC-AP reagent (Vector Lab., Burlingame, CA), and then incubated in the alkaline phosphatase substrate solution. Control samples consisted of sections of tissue from mice treated with nonimmune IgG (Endogen, Boston, MA) or without primary antibody. Tissue sections were counterstained with Gill's hematoxylin in 20% ethylene glycol, and coverslips with Immu-Mount (Shandon, Pittsburgh, PA) were applied. Although all proteases transcripts that have been cloned so far are expressed in the spleen (22), affinity purified anti-mMCP-9 Ig did not recognize any cell in this tissue.

Comparative Protein Modeling and Electrostatic Calculations for mMCP-9—As described for the chymases mMCP-1, mMCP-2, mMCP-4, and mMCP-5 (7), and the tryptases mMCP-6 and mMCP-7 (12, 14), a three-dimensional model of mMCP-9 was built by MODELLER-3[4] (31) with the crystallographic structure of rMCP-II (Brookhaven National Laboratory Protein Data Bank code 3RP2) (6) used as the template. The model of mMCP-9 passes all the stereochemistry checks implemented in the program PROCHECK-3 (32) and also the energy profile test by the program ProsaII (33). The electrostatic potentials of mMCP-9 below and above pH 6.5 were calculated with the GRASP program (34) with standard atomic charges from the CHARMM-22 force field (35). Each Lys and Arg residue was assigned a net positive charge, and each Glu and Asp residue was assigned a net negative charge. Each His residue was assigned a net positive charge below pH 6.5 and a net neutral charge above pH 6.5.

RESULTS

Cloning and Analysis of the mMCP-9 Gene—When the JH-1 genomic clone was digested with *Eco*RI, three fragments were obtained whose sizes were approximately 1.4, 2.6, and 9 kb (Fig. 1*A*). Although the insert in the JH-1 phage clone was only ~13 kb, nucleotide sequencing analysis revealed the presence of two complete serine protease genes. Fragment JH-1A contained exons 1–3 of the mMCP-1 gene, whereas fragment JH-1B contained its last two exons. Based on the conserved exon/intron organization of closely related mMCP genes, the mMCP-9 gene is 2.6 kb in size and contains five exons. Fragment JH-1C contained exons 1–3 of the mMCP-9 gene, whereas fragment JH-1B contained the last two exons of the gene. PCR analysis of the *Eco*RI junctions indicated that the three fragments are contiguous in the isolated phage clone. Moreover, the same sized ~7-kb fragment was isolated from chromosomal and plasmid DNA when a long range PCR approach was used to amplify the nucleotide sequence that spans the two genes (Fig. 1*B*). Thus, the mMCP-1 and mMCP-9 genes are orientated back-to-back with only ~7 kb of 3′ flanking DNA separating them. The nucleotide sequence of the mMCP-9 gene and its exon/intron organization are shown in Fig. 2.

Isolation and Characterization of the mMCP-9 Transcript and Deduced Protein Structure—With primers located in exons 2 and 5 of the mMCP-9 gene, an RT-PCR product of the correct size was obtained from total RNA isolated from the intestines of BALB/c mice that had been infected with *T. spiralis* for 10 days (Fig. 3). The nucleotide sequence of the nearly full-length cDNA corresponded precisely with the putative exons in the gene. The mMCP-9 gene and mRNA, therefore, encode a serine protease whose putative mature form consists of 226 amino acids. In its zymogen form, mMCP-9 has a putative 18-residue signal peptide and a Glu-Glu pro-peptide. In its mature form, mMCP-9 exhibits a >50% overall amino acid sequence identity with the other mMCPs at the complex. mMCP-9 possesses the catalytic triad of His^{45}, Asp^{89}, and Ser^{182}, as well as the N terminus of Ile-Ile-Gly-Gly characteristic of serine proteases. Mature mMCP-9 has two potential *N*-linked glycosylation sites, residing at residues 82 and 100.

Comparative Protein Structure Modeling of mMCP-9—A comparative model of mMCP-9 based on the rMCP-II crystallographic structure revealed that most residues in the S1 sites of mMCP-9, rMCP-II, and pancreatic chymotrypsin are similar in terms of size, polarity, and charge (Fig. 4). Thus, it is likely that mMCP-9 is a chymase, preferring a hydrophobic residue at the P1 position of its substrates. Relative to chymotrypsin, mMCP-9 possesses the same set of insertions and deletions in its amino acid sequence that have been identified in rMCP-II, mMCP-1, mMCP-2, mMCP-4, and mMCP-5. For example, mMCP-9 has the prominent 3-residue insertion in loop A, which extends into the substrate-binding cleft and probably narrows the substrate specificity at the S3′ site. Despite its overall similarity to rMCP-II and the other mouse mast cell chymases, mMCP-9 has a number of unique or nearly unique residues that form its substrate-binding cleft. For example, residue 198 in the substrate-binding cleft is a Ser in mMCP-9 but is a Tyr in most other chymases. There is almost no conservation of the charged residues in the substrate-binding clefts of mMCP-9 and the other mouse mast cell chymases. In particular, mMCP-9 has the most positively charged S3′ site, suggesting a preference for a negatively charged residue at position P3′ in its substrates.

mMCP-9 is the most positively charged mMCP so far cloned. Because mature mMCP-9 possesses 11 Arg, 20 Lys, 7 His, 8 Glu, and 5 Asp residues, it has overall net charges of +25 and +18 at pH values below and above 6.5, respectively. When properly folded, mMCP-9 is predicted to have three almost contiguous regions of positive electrostatic potential that cover approximately one-half of the total molecular surface (Fig. 5). These regions are located away from the substrate-binding cleft. Region 1 includes Lys^{86}, Lys^{118}, Lys^{147}, Lys^{152}, Lys^{155}, Arg^{158}, His^{159}, Lys^{161}, Lys^{173}, Arg^{200}, Lys^{204}, and Arg^{211}. Region 2 includes Lys^{23}, Lys^{24}, Arg^{49}, Arg^{50}, Lys^{69}, Lys^{71}, Lys^{74}, Lys^{94}, Lys^{96}, Lys^{97}, Arg^{221}, and Lys^{224}. Region 3 includes His^{10},

[4] MODELLER is available on Internet at URL http://guitar.rockefeller.edu and also as part of QUANTA and InsightII (MSI, San Diego, CA, USA; E-mail: blp@msi.com).

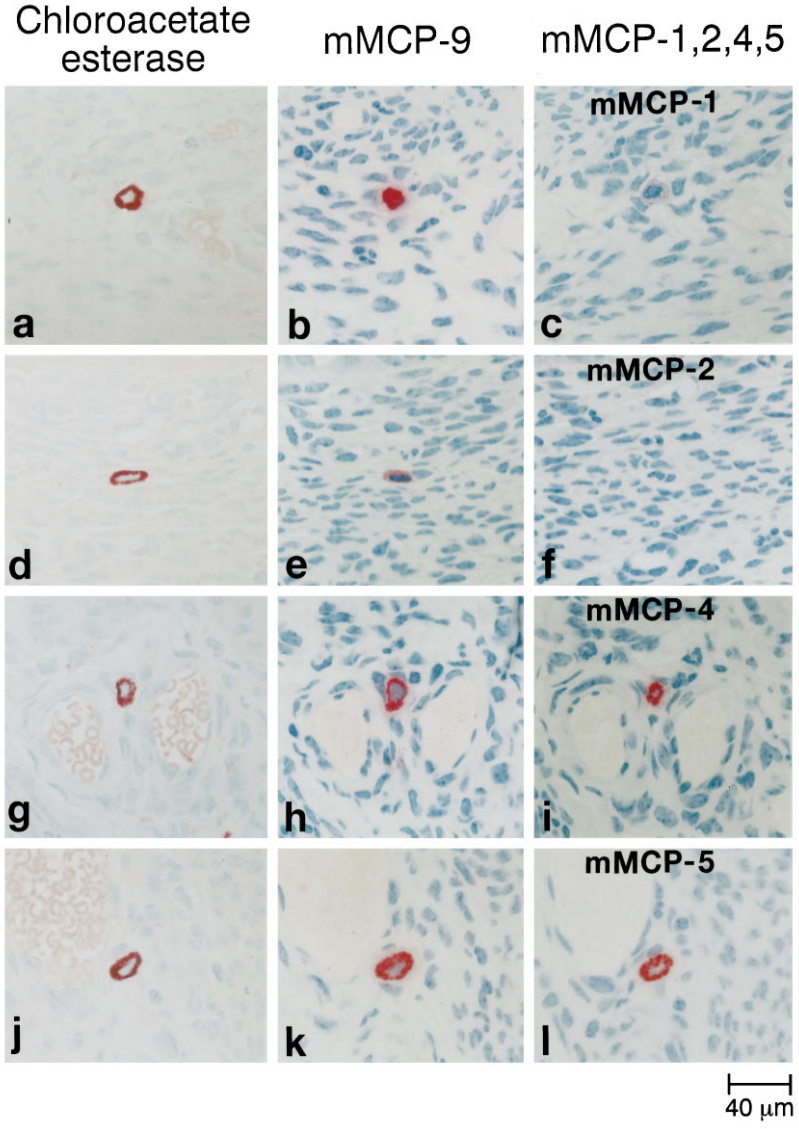

FIG. 7. **Immunohistochemical localization of mMCP-9 in uterine mast cells.** Serial sections (*a-c, d-f, g-i,* and *j-l*) of uterine tissue from normal BALB/c mice were incubated with chloroacetate esterase substrate (*a, d, g,* and *j*), anti-mMCP-9 Ig (*b, e, h,* and *k*), anti-mMCP-1 Ig (*c*), anti-mMCP-2 Ig (*f*), anti-mMCP-4 Ig (*i*), or anti-mMCP-5 Ig (*l*). Each longitudinal section through the uterus contains 11 to 15 chloroacetate esterase-positive mast cells.

Arg^{12}, His^{58}, Arg^{61}, Lys^{62}, Arg^{63}, Arg^{130}, Lys^{134}, Lys^{135}, His^{139}, and Arg^{142}. Because regions 1 and 2 are dominated by Lys and Arg residues, most of the positive charge on these opposing surfaces of mMCP-9 is likely to be maintained when the chymase is exocytosed into a neutral pH environment. However, because of the cluster of three His residues in the center of region 3, a significant reduction of the positive electrostatic potential in region 3 occurs when the pH rises from 5.5 to 7.5 (Fig. 5).

Expression of mMCP-9 in Different Tissues and Populations of Mast Cells—As assessed by RT-PCR analysis, the mMCP-9 transcript is present in those BALB/c mBMMC developed with KL and IL-10 but not in those mBMMC developed with IL-3 (Fig. 6). Whereas the mMCP-9 transcript was not detected in the RNA samples obtained from the ear, intestine, liver, and spleen of normal BALB/c mice, the chymase transcript was detected in RNA samples obtained from the uterus. The mMCP-9 transcript was also detected in RNA samples isolated from the jejunum of BALB/c mice 10 days after infection with *T. spiralis* (Fig. 6). However, blot analysis disclosed that the steady-state level of the mMCP-9 transcript in helminth-infected jejunum is substantially less than that of the induced mMCP-1 transcript (data not shown). The mMCP-9 transcript was not detected in the liver or spleen of the V3 mastocytosis mouse.

Immunohistochemical analysis of serial sectioned tissue from three animals revealed that essentially all of the >100 chloroacetate esterase-positive mast cells examined in the uterus of the normal BALB/c mouse expressed mMCP-9 (Fig. 7). When 20 or more of these mMCP-9-positive cells were analyzed immunohistochemically for the presence of other mMCPs, most uterine mast cells additionally expressed mMCP-4 and mMCP-5. Some expressed a small amount of mMCP-1 but none expressed mMCP-2. As assessed immunohistochemically, the submucosa mast cells are the major population of chloroacetate esterase-positive cells in the mouse jejunum at the height of helminth infection that express mMCP-9 (Fig. 8). These jejunal mast cells also express mMCP-4 and mMCP-5 and, occasionally, mMCP-2; but they rarely, if ever, express mMCP-1. In agreement with the RT-PCR data, mMCP-9 protein was not detected immunohistochemically in the mMCP-5-positive mast cells present in the intestine, spleen, and ear of noninfected mice (data not shown).

DISCUSSION

The analysis of a phage genomic clone revealed the presence of a gene (Fig. 2) that encodes a novel serine protease, designated mMCP-9, residing ~7 kb 3′ of the mMCP-1 gene (Fig. 1). This finding indicates that the chromosome 14 complex in the mouse contains more serine protease genes than previously

recognized. The proximity of the mMCP-1 and mMCP-9 genes also suggests that the low recombination frequency of the complex is a consequence of the closeness of some of its genes. A cluster of five ~3-kb trypsinogen genes has been identified recently in the human β T-cell receptor locus (42). Analogous to the mMCP-1 and mMCP-9 genes, each trypsinogen gene is separated from its adjacent gene by ~7 kb. Thus, this 7-kb spacing may be a common feature for the chromosomal organization of serine protease genes within their individual families.

The β-globin locus is a well studied gene cluster (43). During development, the five genes located in the complex are transcribed in a sequential order with the genes located at the 5′ and 3′ ends of the locus being transcribed first and last, respectively. A locus control element residing ~30 kb 5′ of the embryonic ϵ gene plays a critical role in the regulated expression of these genes (44). The finding by nuclear run-on analysis that most, if not all, chymase genes are transcribed in IL-3-developed BALB/c mBMMC, even though the steady-state levels of the mMCP-1, mMCP-2, and mMCP-4 transcripts are below detection because of a post-transcriptional control mechanism (45), raises the possibility that a distant locus control element promotes the transcription of all mMCP genes at the complex. Mapping studies have revealed that the mouse granzyme B gene is the most 5′ granzyme gene in the chromosome 14 complex. Disruption of this gene does not alter the rate of transcription of the cathepsin G gene but does severely reduce the expression of the other granzymes at the complex (5). Although this finding suggests that transcription of the varied chromosome 14 granzyme genes is regulated by a distant locus control element, it remains to be determined if such an element universally controls the transcription of the chromosome 14 family of chymase genes. The possibility has not been ruled out that the most critical *cis*-acting elements reside at similar sites in the 5′ and/or 3′-flanking regions of each mMCP gene. Nucleotide sequence analysis of its 5′-flanking region revealed that the mMCP-9 gene possesses a putative GATA-binding site at residues −109 to −104, 77 bp upstream of the TATA box (Fig. 2). Mast cells express at least two members of the GATA family of transcription factors (46–48), and the mMCP-1, mMCP-2, mMCP-4, mMCP-5, and mMC-CPA genes all possess a GATA-binding site relatively close to their transcription-initiation sites (3, 15–17, 47). Transient transfection experiments with various reporter constructs have indicated that this GATA site is needed for maximal transcription of the mMC-CPA gene (47). A GATA site 435-bp upstream of its transcription-initiation site also appears to be critical for the expression of a homologous baboon mast cell chymase (48).

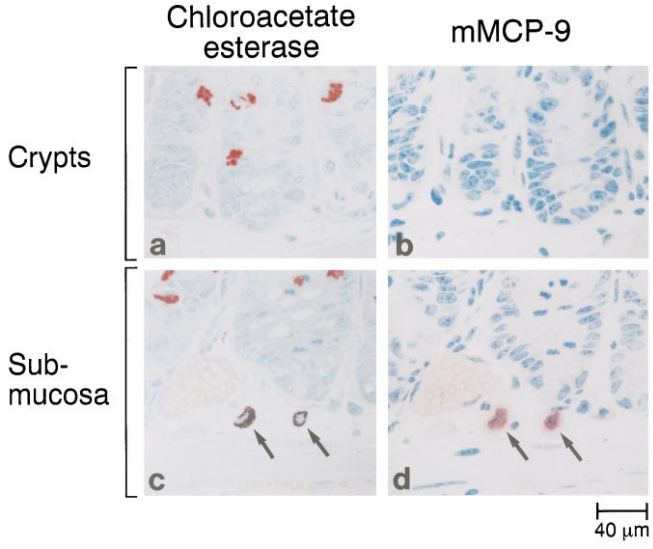

FIG. 8. **Immunohistochemical localization of mMCP-9 in mast cells in the jejunal crypts and submucosa of helminth-infected mice.** Serial sections of the crypts (*a* and *b*) and the submucosa (*c* and *d*) of the jejunum of 10-day *T. spiralis*-infected BALB/c mice were incubated with chloroacetate esterase substrate (*a* and *c*) or anti-mMCP-9 Ig (*b* and *d*). *Arrows* indicate mast cells in the submucosa that express mMCP-9.

Among the chromosome 14 family of mMCPs, the mMCP-5 gene is most dissimilar (Fig. 4 and Table I). Among the more homologous mMCP-1, mMCP-2, mMCP-4, and mMCP-9 genes, the lengths of the individual introns varied somewhat, but their percent identities approach that of the exons. Although ten different serine proteases have been identified in distinct populations of rat mast cells (49–52), none of the cDNAs that encode these proteases seem to be the rat homolog of mMCP-9. Nevertheless, this finding in the rat raises the possibility that additional serine protease genes that have not yet been described reside at the chromosome 14 complex in the mouse.

With primers located in exons 2 and 5 of the mMCP-9 gene, an RT-PCR product of the correct size and nucleotide sequence was obtained from RNA isolated from the intestine of BALB/c mice that had been infected with *T. spiralis* for 10 days (Fig. 3). Based on its deduced amino acid sequence, mMCP-9 encodes a serine protease whose mature form is ~25 kDa. In its zymogen form, mMCP-9 has a hydrophobic signal peptide identical to that in the mMCP-1, mMCP-2, and mMCP-4 zymogens except that an Arg residue replaces a Glu at position −6. Despite the change in net charge, this basic amino acid should not adversely affect the cleavage of the signal peptide in the endoplasmic reticulum because Arg^{-6} is present in the corresponding signal peptides of granzymes B to G (53–55). Like six of the other serine proteases whose genes reside in the chromosome complex, the mMCP-9 zymogen possesses a Glu-Glu pro-peptide. Thus, mMCP-9 probably is activated by the sequential action of serglycin proteoglycans (56) and dipeptidyl peptidase I (57), as observed for a human mast cell chymase and other granule proteases of hematopoietic cells.

Comparative modeling of mMCP-9 (Figs. 4 and 5) suggests that this serine protease is a chymase with a unique and restricted substrate specificity relative to that of chymotrypsin. Mature mMCP-9 is the most positively charged mMCP so far cloned and possesses three positively charged regions on its surface that nearly overlap (Fig. 5). Region 2 is found in all

TABLE I
Homology of the exons and introns of the chromosome 14 family of mMCPs

mMCP	Length and homology of exons and introns[a]								
	Exon 1	Intron 1	Exon 2	Intron 2	Exon 3	Intron 3	Exon 4	Intron 4	Exon 5
mMCP-1	90 (81%)	507 (80%)	151 (85%)	303 (50%)	136 (80%)	198 (76%)	255 (80%)	392 (70%)	396 (65%)
mMCP-2	86 (79%)	492 (79%)	151 (86%)	511 (81%)	136 (73%)	184 (71%)	255 (70%)	354 (64%)	344 (66%)
mMCP-4	91 (92%)	489 (67%)	151 (83%)	503 (75%)	136 (82%)	184 (74%)	255 (77%)	399 (92%)	365 (82%)
mMCP-5	86 (53%)	625 (38%)	151 (65%)	1000 (33%)	136 (62%)	182 (31%)	255 (57%)	328 (43%)	344 (55%)
mMCP-9	91	499	151	529	136	198	255	406	322

[a] The number of nucleotides in each exon and intron of five mMCP genes is indicated as well as their percent identities relative to those in the mMCP-9 gene (parentheses).

mMCPs (7, 12) except mMCP-6 (14). Site-directed mutagenesis revealed that region 2 is the proteoglycan-binding domain of mMCP-7 (12). Region 1 is found in mMCP-4 and mMCP-5 (7), whereas region 3 is found only in mMCP-6 (14). Region 3 of mMCP-9 contains three His residues clustered in its center. Thus, this region is predicted to lose some of its positive electrostatic potential once mMCP-9 is exocytosed from the mast cell into a neutral pH environment (Fig. 5*B*). Recent analysis of mMCP-5-null mice has suggested that region 1 is used by mMCP-5 to form a binary complex with the negatively charged pro-peptide of mMC-CPA to ensure that the two proteases are targeted to the secretory granules of cutaneous mast cells in equimolar amounts (58). Thus, it is likely that mMCP-9 also uses these positively charged regions to form multimeric complexes with serglycin proteoglycans and other negatively charged proteins inside, and possibly outside, the mast cell.

mMCP-9 transcript (Fig. 6) and protein (Fig. 7) are abundant in the uterus of the normal BALB/c mouse. Mast cells and their mediators have been implicated in the development of the mouse uterus (59–61). Because certain mast cell chymases have been implicated in the degradation of extracellular matrices, mMCP-9 may play a role in the tissue remodeling of the uterus during pregnancy or the normal estrous cycle. The mMCP-9 transcript (Fig. 6) and/or protein were not detected in the ear, liver, spleen, or intestine of normal BALB/c mice and were not detected in cultured V3 mast cells or in the more mature V3 mast cells that develop in the spleen and liver of BALB/c mice after adoptive transfer. Because all other chymases are expressed in spleen and liver of the mastocytosis mouse (22), the expression of mMCP-9 is among the most restricted of the other known chymases.

The mMCP-9 transcript was not detected in the jejunum of uninfected animals but was found in the jejunum of BALB/c mice 10 days after *T. spiralis* infection (Figs. 3 and 6) when jejunal mast cells are abundant (21). However, blot analysis revealed that the steady-state level of the mMCP-9 transcript was substantially less than that of the mMCP-1 transcript. Although mast cells are found in the muscle and submucosa regions of the jejunum at the height of helminth infection, ~90% of the mast cells in the jejunum reside in the lamina propria and epithelium. Immunohistochemical analysis revealed that mMCP-9 is expressed by the mMCP-5-positive mast cells in the submucosa (Fig. 8), whereas mMCP-1 is expressed by the larger number of mMCP-5-negative mast cells in the lamina propria and epithelium (21, 36, 37). This observation is compatible with the mMCP-9 transcript being less abundant than the mMCP-1 transcript in the RNA sample obtained from the entire jejunum. The observation that mMCP-9 is expressed by BALB/c mBMMC developed in the presence of KL and IL-10 but not by those developed in the presence of IL-3 alone (Fig. 6) indicates that the expression of this chymase is selectively regulated by the cytokine microenvironment around the cell.

REFERENCES

1. Brunet, J. F., Dosseto, M., Denizot, F., Mattei, M. G., Clark, W. R., Haqqi, T. M., Ferrier, P., Nabholz, M., Schmitt-Verhulst, A. M., Luciani, M. F., and Golstein, P. (1986) *Nature* **322,** 268–271
2. Crosby, J. L., Bleackley, R. C., and Nadeau, J. H. (1990) *Genomics* **6,** 252–259
3. Gurish, M. F., Nadeau, J. H., Johnson, K. R., McNeil, H. P., Grattan, K. M., Austen, K. F., and Stevens, R. L. (1993) *J. Biol. Chem.* **268,** 11372–11379
4. Heusel, J. W., Scarpati, E. M., Jenkins, N. A., Gilbert, D. J., Copeland, N. G., Shapiro, S. D., and Ley, T. J. (1993) *Blood* **81,** 614–1623
5. Pham, C. T. N., MacIvor, D. M., Hug, B. A., Heusel, J. W., and Ley, T. J. (1996) *Proc. Natl. Acad. Sci. U. S. A.* **93,** 13090–13095
6. Remington, S. J., Woodbury, R. G., Reynolds, R. A., Matthews, B. W., and Neurath, H. (1988) *Biochemistry* **27,** 8097–8105
7. Šali, A., Matsumoto, R., McNeil, H. P., Karplus, M., and Stevens, R. L. (1993) *J. Biol. Chem.* **268,** 9023–9034
8. Murphy, M. E., Moult, J., Bleackley, R. C., Gershenfeld, H., Weissman, I. L., and James, M. N. (1988) *Proteins* **4,** 190–204
9. De Young, M. B., Nemeth, E. F., and Scarpa, A. (1987) *Arch. Biochem. Biophys.* **254,** 222–233
10. McNeil, H. P., Reynolds, D. S., Schiller, V., Ghildyal, N., Gurley, D. S., Austen, K. F., and Stevens, R. L. (1992) *Proc. Natl. Acad. Sci. U. S. A.* **89,** 11174–11178
11. Johnson, D. A., and Barton, G. J. (1992) *Protein Sci.* **1,** 370–377
12. Matsumoto, R., Šali, A., Ghildyal, N., Karplus, M., and Stevens, R. L. (1995) *J. Biol. Chem.* **270,** 19524–19531
13. Reynolds, D. S., Gurley, D. S., Austen, K. F., and Serafin, W. E. (1991) *J. Biol. Chem.* **266,** 3847–3853
14. Ghildyal, N., Friend, D. S., Stevens, R. L., Austen, K. F., Huang, C., Penrose, J., Šali, A., and Gurish, M. F. (1996) *J. Exp. Med.* **184,** 1061–1073
15. Huang, R., Blom, T., and Hellman, L. (1991) *Eur. J. Immunol.* **21,** 1611–1621
16. Serafin, W. E., Sullivan, T. P., Conder, G. A., Ebrahimi, A., Marcham, P., Johnson, S. S., Austen, K. F., and Reynolds, D. S. (1991) *J. Biol. Chem.* **266,** 1934–1941
17. McNeil, H. P., Austen, K. F., Somerville, L. L., Gurish, M. F., and Stevens, R. L. (1991) *J. Biol. Chem.* **266,** 20316–20322
18. Sanger, F., Nicklen, S., and Coulson, A. R. (1977) *Proc. Natl. Acad. Sci. U. S. A.* **74,** 5463–5467
19. Reynolds, D. S., Stevens, R. L., Lane, W. S., Carr, M. H., Austen, K. F., and Serafin, W. E. (1990) *Proc. Natl. Acad. Sci. U. S. A.* **87,** 3230–3234
20. Ghildyal, N., McNeil, H. P., Stechschulte, S., Austen, K. F., Silberstein, D., Gurish, M. F., Somerville, L. L., and Stevens, R. L. (1992) *J. Immunol.* **149,** 2123–2129
21. Friend, D. S., Ghildyal, N., Austen, K. F., Gurish, M. F., Matsumoto, R., and Stevens, R. L. (1996) *J. Cell Biol.* **135,** 279–290
22. Gurish, M. F., Pear, W. S., Stevens, R. L., Scott, M. L., Sokol, K., Ghildyal, N., Webster, M. J., Hu, X., Austen, K. F., Baltimore, D., and Friend, D. S. (1995) *Immunity* **3,** 175–186
23. Razin, E., Ihle, J. N., Seldin, D., Mencia-Huerta, J-M., Katz, H. R., LeBlanc, P. A., Hein, A., Caulfield, J. P., Austen, K. F., and Stevens, R. L. (1984) *J. Immunol.* **132,** 1479–1486
24. Murakami, M., Austen, K. F., Bingham, C. O., III, Friend, D. S., Penrose, J. F., and Arm, J. P. (1995) *J. Biol. Chem.* **270,** 22653–22656
25. Chomczynski, P., and Sacchi, N. (1987) *Anal. Biochem.* **162,** 156–159
26. Alonso, S., Minty, A., Bourlet, Y., and Buckingham, M. (1986) *J. Mol. Evol.* **23,** 11–22
27. Boenisch, T., Farmilo, A. J., and Stead, R. H. (1989) in *Immunochemical Staining Methods Handbook* (Naish, S. J., ed), p. 11, DAKO Corp., Carpinteria, CA
28. Ghildyal, N., Friend, D. S., Nicodemus, C. F., Austen, K. F., and Stevens, R. L. (1993) *J. Immunol.* **151,** 3206–3214
29. McNeil, H. P., Frenkel, D. P., Austen, K. F., Friend, D. S., and Stevens, R. L. (1992) *J. Immunol.* **149,** 2466–2472
30. Beckstead, J. H., Halverson, P. S., Ries, C. A., and Bainton, D. F. (1981) *Blood* **57,** 1088–1098
31. Šali, A., and Blundell, T. L. (1993) *J. Mol. Biol.* **234,** 779–815
32. Laskowski, R. L., McArthur, M. W., Moss, D. S., and Thornton, J. M. (1993) *J. Appl. Crystallogr.* **26,** 283–291
33. Sippl, M. J. (1993) *Proteins* **17,** 355–362
34. Nicholls, A., Sharp, K. A., and Honig, B. (1991) *Proteins* **11,** 281–296
35. Brooks, B. R., Bruccoleri, R. E., Olafson, B. D., States, D. J., Swaminathan, S., and Karplus, M. K. (1983) *J. Comp. Chem.* **4,** 187–217
36. Serafin, W. E., Reynolds, D. S., Rogelj, S., Lane, W. S., Conder, G. A., Johnson, S. S., Austen, K. F., and Stevens, R. L. (1990) *J. Biol. Chem.* **265,** 423–429
37. Le Trong, H., Newlands, G. F. J., Miller, H. R. P., Charbonneau, H., Neurath, H., and Woodbury, R. G. (1989) *Biochemistry* **28,** 391–395
38. Woodbury, R. G., Katunuma, N., Kobayashi, K., Titani, K., and Neurath, H. (1978) *Biochemistry* **17,** 811–819
39. Mikeš, O., Holeyšovský, V., Tomášek, V., and Šorm, F. (1966) *Biochem. Biophys. Res. Commun.* **24,** 346–352
40. Meloun, B., Kluh, I., Kostka, V., Morávek, L., Prusík, Z., Vaněček, J., Keil, B., and Šorm, F. (1966) *Biochim. Biophys. Acta* **130,** 543–546
41. Perona, J. J., and Craik, C. S. (1995) *Protein Sci.* **4,** 337–360
42. Rowen, L., Koop, B. F., and Hood, L. (1996) *Science* **272,** 1755–1762
43. Evans, T., Felsenfeld, G., and Reitman, M. (1990) *Annu. Rev. Cell Biol.* **6,** 95–124
44. Grosveld, F., van Assendelft, G. B., Greaves, D. R., and Kollias, G. (1987) *Cell* **51,** 975–985
45. Xia, Z., Ghildyal, N., Austen, K. F., and Stevens, R. L. (1996) *J. Biol. Chem.* **271,** 8747–8753
46. Martin, D. I. K., Zon, L. I., Mutter, G., and Orkin, S. H. (1990) *Nature* **344,** 444–437
47. Zon, L. I., Gurish, M. F., Stevens, R. L., Mather, C., Reynolds, D. S., Austen, K. F., and Orkin, S. H. (1991) *J. Biol. Chem.* **266,** 22948–22953
48. Liao, Y., Yi, T., Hoit, B. D., Walsh, R. A., Karnik, S. S., and Husain, A. (1997) *J. Biol. Chem.* **272,** 2969–2976
49. Woodbury, R. G., Katunuma, N., Kobayashi, K., Titani, K., and Neurath, H. (1978) *Biochemistry* **17,** 811–819
50. Le Trong, H., Parmelee, D. C., Walsh, K. A., Neurath, H., and Woodbury, R. G. (1987) *Biochemistry* **26,** 6988–6994
51. Benfey, P. N., Yin, F. H., and Leder, P. (1987) *J. Biol. Chem.* **262,** 5377–5384
52. Lützelschwab, C., Pejler, G., Aveskogh, M., and Hellman, L. (1996) *J. Exp. Med.* **185,** 13–29
53. Lobe, C. G., Upton, C., Duggan, B., Ehrman, N., Letellier, M., Bell, J., McFadden, G., and Bleackley, R. C. (1988) *Biochemistry* **27,** 6941–6946
54. Jenne, D., Rey, C., Haefliger, J-A., Qiao, B-Y., Groscurth, P., and Tschopp, J. (1988) *Proc. Natl. Acad. Sci. U. S. A.* **85,** 4814–4818
55. Jenne, D., Rey, C., Masson, D., Stanley, K. K., Herz, J., Plaetinck, G., and Tschopp, J. (1988) *J. Immunol.* **140,** 318–323
56. Murakami, M., Karnik, S. S., and Husain, A. (1995) *J. Biol. Chem.* **270,** 2218–2223
57. McGuire, M. J., Lipsky, P. E., and Thiele, D. L. (1993) *J. Biol. Chem.* **268,**

2458–2467
58. Stevens, R. L., Qui, D., McNeil, H. P., Friend, D. S., Hunt, J. E., Austen, K. F., and Zhang, J. (1996) *FASEB J.* **10,** 1307
59. Hughes, M. J., Lingrel, J. B., Krakowsky, J. M., and Anderson, K. P. (1993) *J. Biol. Chem.* **268,** 20687–20690
60. Stechschulte, D. J., Sharma, R., Dileepan, K. N., Simpson, K. M., Aggarawal, N., Clancy, J., Jr., and Jilka, R. L. (1987) *J. Cell. Physiol.* **132,** 565–570
61. Yokoi, H., Nakayama, H., Horie, K., Fukumoto, M., Fujita, K., Kaneko, Y., Iwai, M., Natsuyama S., Kanzaki, H., Mori, K. J., and Fujita, J. (1994) *Biol. Reprod.* **50,** 1034–1039